

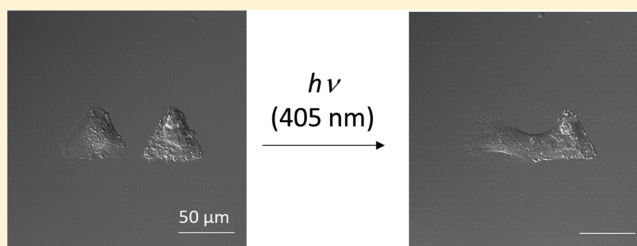
# Sequential Photoactivation of Self-Assembled Monolayers to Direct Cell Adhesion and Migration

Pradeep Bugga and Milan Mrksich\*<sup>1b</sup>

Department of Chemistry, Department of Biomedical Engineering, and Department of Cell and Molecular Biology, Northwestern University, Evanston, Illinois 60208, United States

## Supporting Information

**ABSTRACT:** Dynamic substrates for cell culture control the spatial and temporal presentation of extracellular matrix ligands that interact with adherent cells. This paper reports a photoactive surface chemistry that can repeatedly activate regions of the substrate for cell adhesion, spreading, and migration. The approach uses self-assembled monolayers presenting the integrin ligand RGD that is caged with a nitrophenyl-based photoprotecting group. The group is also modified with a maltoheptaose oligosaccharide to prevent nonspecific protein adsorption and cell attachment. The peptide is uncaged when irradiated with a laser source at 405 nm on a microscope to reveal micron-size regions for single cell attachment. This method is applied to studies of gap junction-mediated communication between two neighboring cells and requires the patterning of an initial receiver cell population and then the patterning of a second sender population to give a culture wherein each pair of cells are separated by 30  $\mu\text{m}$ . Finally, activation of the region between the cells permits cell–cell contact and gap junction assembly between the sender and receiver cells. This example demonstrates the broad relevance of this method to studying complex phenotypes in cell culture.



## INTRODUCTION

The development of model substrates that present extracellular matrix (ECM) ligands has been important in studying cell adhesion, migration, and differentiation.<sup>1–4</sup> Dynamic substrates in particular—where the activities of ligands can be switched on and off during cell culture—have provided an exciting strategy to mimic the dynamic aspects of biological ECM.<sup>5–9</sup> Most of the methods used to control the activities of ligands are based on electrochemical, thermal, or magnetic modulation and have the limitation that they do not offer unrestricted spatio-temporal control over ligand activity.<sup>10–13</sup> In this paper, we describe dynamic substrates based on a photocaged adhesion ligand, and we demonstrate high resolution, *in situ*, and completely flexible control over the timing and position of ligand activation. Furthermore, we describe an application of this strategy to studies of gap junction-mediated cell–cell communication.

Many surface and polymer chemistries are available for preparing dynamic substrates that can modulate the activities of ligands, and those based on self-assembled monolayers (SAMs) of alkanethiolates on gold have been among the most effective.<sup>14,15</sup> SAMs are structurally well-defined and offer wide synthetic flexibility in controlling the structures and properties of the surface, including a host of immobilization chemistries for controlling the densities, orientations, and patterns of adhesion ligands. Further, monolayers that present oligo-(ethylene glycol) groups are among the most effective at preventing the nonspecific adsorption of protein (and attachment of cells) and, therefore, in controlling ligand–

receptor interactions with an adherent cell.<sup>16</sup> Photochemical strategies have offered the greatest flexibility in spatio-temporal manipulation of a substrate. The Nakanishi group, for example, demonstrated an approach wherein a monolayer functionalized with a photoprotected carboxylate resisted cell adhesion because of an adsorbed layer of bovine serum albumin (BSA).<sup>17</sup> Irradiation at 365 nm resulted in uncaging of the acid and desorption of BSA, which then permitted adsorption of exogenously added fibronectin for cell attachment and migration. In a similar strategy, this group coimmobilized a photocleavable poly(ethylene glycol) chain and a cyclic RGD peptide and demonstrated that the inert substrate could be switched to cell adhesive after irradiation.<sup>18</sup> In another approach, Yousaf and Park uncaged a nitroveratryloxycarbonyl-protected group for subsequent immobilization of the RGD peptide by way of an oxime linkage.<sup>19</sup> Del Campo and co-workers designed a surface presenting a photocaged RGD ligand and demonstrated the patterning of cells and subsequent activation of the surface to initiate cell migration.<sup>20</sup> This latter example represents the most effective route for photomodulation of a surface for cell adhesion, but it does require the use of a blocking protein that may limit the number of times the surface can be activated. In this report, we use a monolayer that presents a photoprotected RGD ligand modified with an oligosaccharide to prevent nonspecific

Received: December 18, 2018

Revised: March 28, 2019

Published: April 3, 2019

protein adsorption and that also allows multiple cycles of photoactivation of the monolayer. Importantly, we describe how the introduction of a photocaging group onto the RGD ligand resulted in significant nonspecific attachment of cells, and we show that the modification of this caging group with an oligosaccharide served to maintain inertness of the monolayer. We demonstrate the benefit of this approach by sequentially patterning two distinct populations of cells and then initiating a cell–cell junction to study transcellular transport.

## RESULTS AND DISCUSSION

**Design.** Our approach for repeatedly patterning regions of a substrate for cell attachment uses a SAM that presents a photoprotected RGD ligand against an otherwise inert background (Figure 1). We prepared the surfaces by

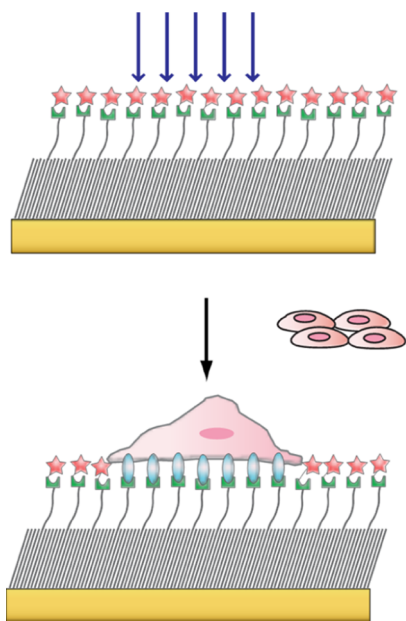


**Figure 1.** Monolayer presenting photocaged RGD adhesion ligands (red star) against an otherwise inert background is photodeprotected to reveal the ligands (green block), which then allows cell adhesion and spreading.

immobilizing a photoprotected RGD ligand to a monolayer that presents maleimide groups against a background of tri(ethylene glycol) groups (Figure 2). The latter group is effective at preventing nonspecific protein adsorption and ensuring cell attachment is exclusively mediated by the RGD peptide.<sup>16</sup>

The RGD peptide was photocaged with a 3-(4,5-dimethoxy-2-nitrophenyl)-2-butyl ester (DMNPB) protecting group at the aspartic acid side chain, as reported by del Campo and co-workers.<sup>20</sup> The group is efficiently removed when irradiated at 405 nm on a confocal microscope and, therefore, can be used to pattern monolayers with micrometer resolution for cell attachment. Importantly, the surface can be repeatedly photoactivated and imaged with optical/fluorescent microscopy to observe cell adhesion and enable more complex cell culture experiments. As we show in the work that follows, we not only pattern two cell types with single cell resolution, but we also subsequently activate regions between the patterned cells to initiate cell–cell contact in a defined geometry.

**Preparation of Monolayers.** We prepared SAMs that presented maleimide groups at densities of 0.1–1% against a background of tri(ethylene glycol) groups as described previously.<sup>21</sup> We synthesized the photoprotected RGD ligand, cyclic RGD(DMNPB)fC, using standard Fmoc peptide synthesis protocols with DMNPB-protected Fmoc-L-aspartate. We chose the cyclic form of the peptide (as opposed to the common linear form) because much work has established that it is a better mimic of native ECM compared to the lower affinity linear form.<sup>22,23</sup> We used self-assembled monolayers for matrix-assisted laser desorption ionization-mass spectrometry (SAMDI-MS) to confirm immobilization of the protected peptide (Figure S1) because this technique provides masses for the alkanethiolates in the monolayer.<sup>24</sup> Peaks in the spectrum corresponded to the expected masses for the peptide–alkanethiolate conjugate as a mixed disulfide with the tri(ethylene glycol)-terminated chain (1666  $m/z$ ) as well as the free alkanethiolate (1332  $m/z$ ). We also observed peaks corresponding to photodegradation products including loss of the photoprotecting group (−237 Da) and fragmentation of the nitro group (−16 Da). The mass spectrometer uses a 355 nm laser to desorb the monolayer, and this wavelength overlaps with the absorption spectrum for the nitrophenyl chromophore and is therefore expected to cause at least partial

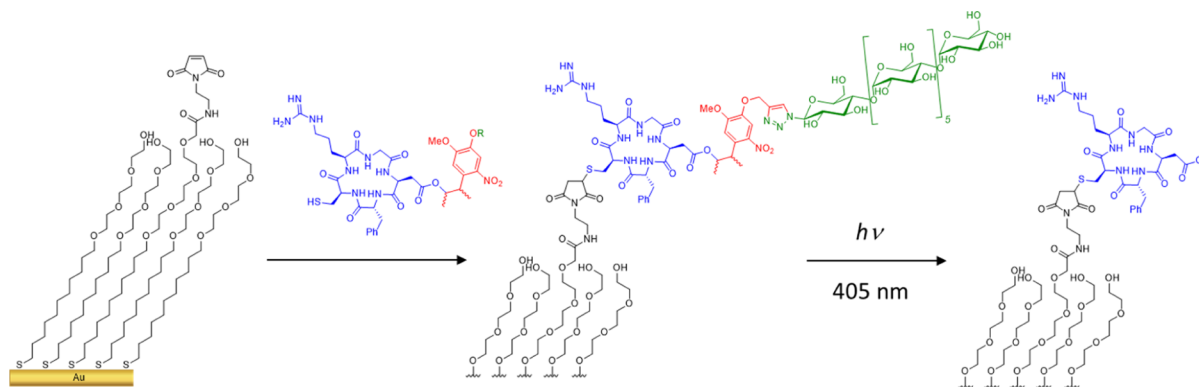


**Figure 2.** Monolayer presenting maleimide groups against a background of tri(ethylene glycol) groups was treated with a cyclic RGD peptide (blue) having a photoprotecting group (red) at the aspartic acid side chain and a cysteine that allowed its covalent immobilization to the monolayer. Irradiation of the monolayer at 405 nm results in deprotection of the peptide and can be used to activate select regions of the monolayer for cell adhesion. As described later, the oligosaccharide chain (green) on the photoprotecting group renders the surface inert and allows repeated cycles of activation.

deprotection of the peptide. Indeed, a regular matrix-assisted laser desorption ionization spectrum of the free peptide reveals peaks at the corresponding mass, confirming that the fragmentation is not influenced by the SAM structure (Figure S1).

#### Photoactivation of the Monolayer for Cell Adhesion.

To test our ability to switch cell adhesion with our DMNPB photoprotected RGD monolayer, we optimized photodeprotection with a 365 nm UV lamp source (Figure S2) and then cultured cells on this monolayer with and without irradiation. We observed poorly attached cells on photoprotected surfaces but well-spread cells on the UV-treated surfaces comparable to that observed on monolayers presenting the unprotected RGD ligand (Figure S3). Thereafter, we used a confocal microscope equipped with a diode laser at 405 nm along with the manufacturer's software designed to perform photobleaching experiments to activate regions of the monolayer for cell adhesion. We first performed several experiments to determine the combination of write speed and laser intensity that gives complete deprotection of the peptide; in this way, we could minimize the time needed for patterning and also minimize any unwanted damage to the monolayer that might stem from the excess irradiation. We programmed the microscope to deprotect a millimeter-sized square by rastering the region in a serpentine pattern. We repeated this process for laser energy densities ranging from 0.5 to 25 J/cm<sup>2</sup>. We first found that illumination at 1 J/cm<sup>2</sup>, with a dwell time of ~20  $\mu$ s, gave complete deprotection (Figure 3). Reducing the irradiation

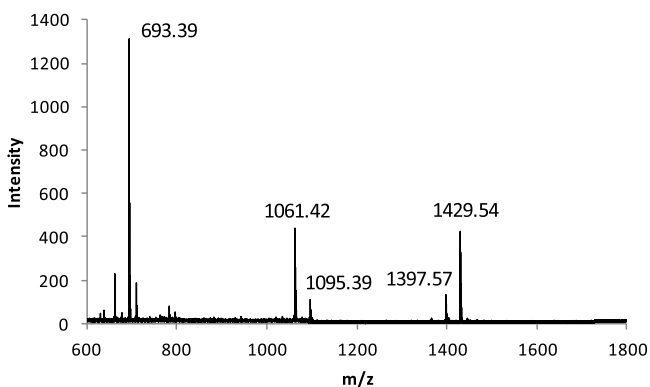


**Figure 3.** SAMDI mass spectrum of a monolayer presenting a photoprotected RGD ligand after irradiation with a 405 nm laser at 1 J/cm<sup>2</sup>. The expected peaks for the photoprotected RGD-terminated alkanethiolates at 1666  $m/z$  and 1332  $m/z$  are not present, whereas the corresponding peaks for the deprotected peptide, at 1429  $m/z$  and 1095  $m/z$ , are present.

time by a factor of 2 still gave >90% deprotection of the peptide (as defined by the ratio of the areas under the curves for peaks corresponding to the deprotected peptide and the sum of the areas under the curves for peaks corresponding to both the protected and deprotected peptide) (Figure S4). In the experiments that follow, we used a laser energy density of 1 J/cm<sup>2</sup> and a dwell time of 20  $\mu$ s to pattern monolayers.

We next patterned a monolayer supported on a glass coverslip coated with an optically transparent film of gold and where the photocaged RGD peptide was present at a density of 1% relative to the tri(ethylene glycol) groups. We programmed the microscope to pattern the slide with a 10  $\times$  11 array of rectangular features, each measuring 22  $\mu$ m  $\times$  44  $\mu$ m and each spaced from its neighbor by 100  $\mu$ m. We then allowed HT-

1080 fibrosarcoma cells to attach to the substrate for 1 h before exchanging the medium and incubating the cells at 37  $^{\circ}$ C for ~8 h (Figure 4). Optical micrographs reveal that cells were

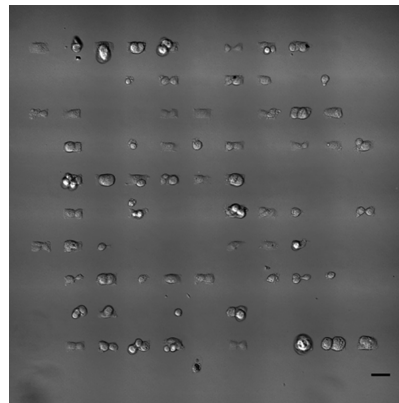


**Figure 4.** Monolayer presenting DMNPB photoprotected RGD was patterned with a microscope laser into an array of 22  $\mu$ m  $\times$  44  $\mu$ m rectangular regions. HT-1080 cells were seeded and cultured for 8 h. An optical micrograph shows that cells selectively attached to and spread within illuminated regions. Scale bar—50  $\mu$ m.

confined to the patterned rectangular features, confirming that the deprotected regions serve as a matrix for cell adhesion and that the complementary photoprotected regions could still prevent nonspecific cell attachment. The number of patterned regions not having an attached cell can be reduced by increasing the number of suspended cells present during adhesion or allowing adhesion to continue with a second batch of suspended cells.

**Inertness of Monolayers Presenting Photocaged RGD.** In experiments that pattern two different cell populations, it is necessary to pattern the first population and then to perform a second patterning step to place the second cell population. Hence, the regions that are not deprotected in the first step must remain inert to cell attachment during the intervening steps and then must still be able to be deprotected and support attachment. However, our early experiments revealed that the second population of cells failed to attach to the patterns that were activated in a second photopatterning step (Figure 5). We reasoned that the second patterning step failed because the monolayer was no longer inert to the nonspecific adsorption of protein and that adsorption of protein would block the RGD peptides and prevent cell adhesion. Specifically, adsorption of BSA, a major component of cell culture media, could prevent cell adhesion to regions of the surface that had deprotected RGD ligands.

To address this possibility, we used surface plasmon resonance (SPR) spectroscopy to directly characterize the adsorption of BSA onto monolayers presenting DMNPB photoprotected RGD as well as a control monolayer presenting only the tri(ethylene glycol) group (Figure 6). We prepared monolayers on gold-coated coverslips and mounted these substrates into cassettes from the manufacturer, as described previously.<sup>25</sup> Phosphate-buffered saline (PBS) buffer was allowed to flow over the chip for 2 min, then a solution of BSA in PBS (1 mg/mL) for 25 min, and finally PBS buffer again for 10 min. Figure 6 shows that there was essentially no adsorption of BSA to monolayers that presented only the tri(ethylene glycol) group—that is, monolayers that had the photoprotected peptide present at a density of 0%—whereas a



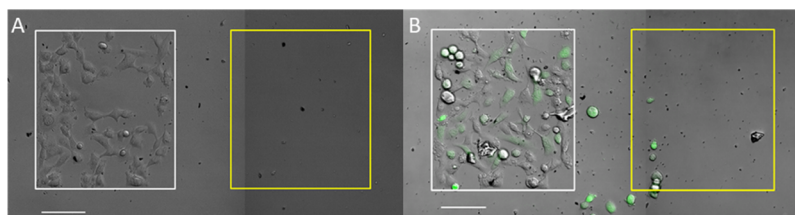


**Figure 5.** Monolayer of DMNPB photoprotected RGD was photopatterned with a  $300\ \mu\text{m} \times 350\ \mu\text{m}$  region (white) and then HT-1080 cells were cultured for 3–4 h. A second region (yellow) was thereafter illuminated, followed by culturing of a second population of cells dyed with CellTracker Green. Overlaid bright-field and fluorescent images show that the first population of cells selectively attaches and spreads to the illuminated region (A). The second population (green) also attaches and spreads to the first region but fails to do so to the second region (B). Scale bar— $100\ \mu\text{m}$ .

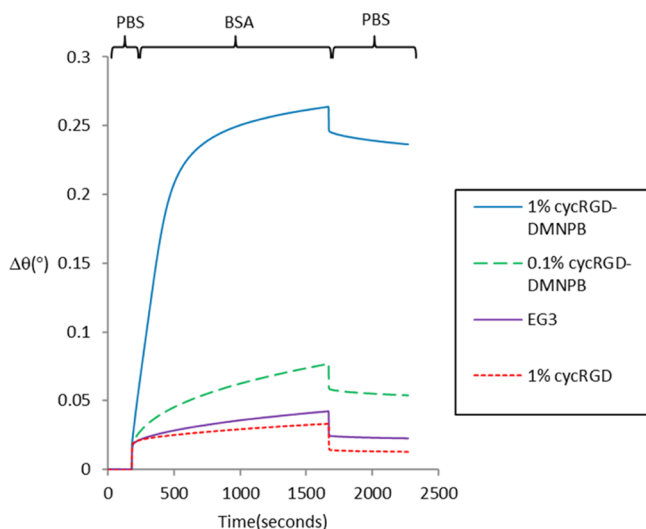


**Figure 6.** Data from SPR spectroscopy for the adsorption of BSA (1 mg/mL in pH 7.6 PBS buffer) to monolayers presenting photoprotected RGD at a density of 1% (top), 0.1% (second from top), a monolayer having the unprotected RGD at a density of 1% (bottom), and a monolayer of tri(ethylene glycol) (third from top). The change in angle of minimum reflectivity ( $\Delta\theta$ ) is plotted against time as solutions are allowed to flow over the surface. PBS buffer was first allowed to flow, followed by a solution of protein in buffer and then buffer. The periods of time during which each solution was allowed to flow over the monolayer are indicated above the plot.

modest amount of protein adsorbed to the monolayer with the protected peptide present at 0.1% density and a substantial amount of protein adsorbed to monolayers having a peptide present at a density of 1%. This latter amount corresponds to the amount of adsorption observed on a methyl-terminated monolayer ( $\Gamma_{\text{CH}_3} = 210\ \text{ng}/\text{cm}^2$  vs  $\Gamma_{\text{RGD}} = 212\ \text{ng}/\text{cm}^2$ ) and represents a near-complete monolayer of protein.<sup>26</sup> Hence, the presence of the photoprotected peptide, even at densities of only 1%, compromises the inertness of the monolayer and gives near maximum nonspecific adsorption of protein. Finally, we confirmed this lack of inertness by observing that under serum-free conditions (without BSA), cells nonspecifically attach to a monolayer presenting protected RGD peptide at a density of 1% (Figure S5). These properties are consistent with our observation that when patterning two cell populations, the first population is able to attach to the regions that are initially deprotected (and before any protein was introduced to the monolayer), but subsequent cell attachment is inhibited by the adsorbed layer of protein.

**Inertness of Monolayers Presenting RGD with a Modified Photoprotecting Group.** To address this loss of inertness, we modified the DMNPB photoprotecting group to include an oligosaccharide; prior work has shown that carbohydrates are effective at preventing nonspecific protein adsorption,<sup>27,28</sup> and work by Micklefield and co-workers showed that photoprotecting groups could be rendered more inert when modified with groups that are normally used to make surfaces inert [i.e., an oligo(ethylene glycol) group].<sup>29</sup> We synthesized a new protecting group wherein one methoxy

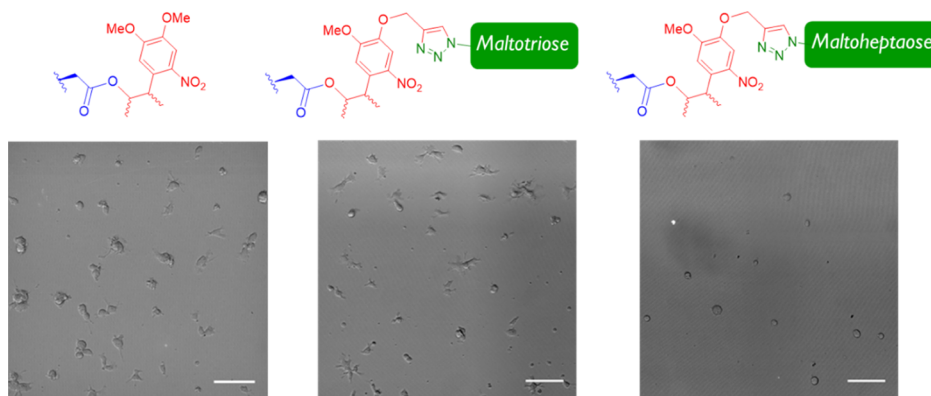


**Figure 7.** Monolayers presenting RGD with DMNPB (left), maltotriose-clicked (middle), and maltoheptaose-clicked photoprotecting groups were prepared at 0.1% density. HUVEC cells were seeded on surfaces in serum-free media to determine the inertness of the various surfaces to nonspecific cell attachment. Optical micrographs reveal that while the maltotriose surface still promoted adhesion, the maltoheptaose surface was sufficiently inert for carrying out repeated photoactivation experiments. Scale bar— $100\ \mu\text{m}$ .

group of the nitrophenyl core was substituted with a propargyl ether and which therefore provided a handle to introduce azido-carbohydrates by way of a click reaction. The synthesis of this molecule is described in [Scheme S1](#), and after preparing a protected Asp Fmoc amino acid, we synthesized a cyclic RGD peptide protected with this new group. To this alkyne-containing peptide, we coupled either  $\beta$ -D-maltotriose azide or  $\beta$ -D-maltoheptaose azide (both prepared via a one-step “Shoda activation”).<sup>30</sup> We then immobilized the resulting peptides to the maleimide-terminated monolayers, and we confirmed immobilization using SAMDI-MS ([Figure S6](#)). Next, we tested the effect of including the oligosaccharide in the photoprotecting group by measuring nonspecific cell attachment on monolayers presenting these two peptides along with the first-generation DMNPB-protected peptide ([Figure 7](#)). The maltotriose conjugate slightly improved inertness, and the maltoheptaose conjugate was substantially more effective. Finally, monolayers presenting the maltoheptaose-containing peptide at low density (0.1%) completely reduced nonspecific cell attachment for human umbilical vein endothelial cells (HUVECs). This low density was required as surfaces presenting this peptide higher than 0.1% density were not inert. The observation that the inclusion of an oligosaccharide in the photoprotecting group could improve inertness is also supported by SPR data showing a reduction in BSA adsorption with the maltotriose conjugate ([Figure S7](#)). We used the maltoheptaose photoprotected monolayer for patterning experiments described next.

**Gap Junction Dynamics.** We used the monolayers described above to pattern two populations of HUVECs to visualize transport of cytosolic molecules through gap junctions formed between neighboring cells. This example required the patterning of pairs of single cells—where the first was labeled with a fluorescent dye in order to visualize diffusion through the gap junction—with a separation between the cells of  $\sim 30 \mu\text{m}$ . We chose HUVECs because of their significant expression of the gap junction connexin protein. Additionally, we fabricated a “monolayer-bottom” culture chamber with three-dimensional printing to obtain high-quality fluorescent images ([Figure S8](#)). We first patterned the monolayer with an array of triangular features and allowed HUVECs to attach to these features for 4–5 h, which resulted in an array of cells that were attached to the triangular shapes. We then patterned a second set of triangular features adjacent to the first, with a center-to-center spacing of  $75 \mu\text{m}$ , and allowed cells preloaded with calcein-acetoxymethyl (AM) dye to attach to these features. We optimized the distance between the pairs of triangular features to prevent migration of the first cell into the second illuminated region but still allow activation of gap junction assembly between the neighboring cells. We subsequently observed efficient attachment of the second population that assumed shapes that again mirrored the pattern ([Figure 8](#)). After 2–3 h in culture, we performed a third photopatterning step where we illuminated the gap region between each pair of cells. Thereafter, we used bright-field microscopy to observe interaction of the cells and fluorescence microscopy to image transport and diffusion of the dye from the first cell to the second ([Movie S1](#)).

Once the middle region was activated, we observed protrusions from the vertices of the triangular cells that gave cell–cell contact within a few hours, and clear diffusion of the dye about 3 h later. Transfer of the calcein dye occurred after cell–cell contact and is consistent with the assembly of

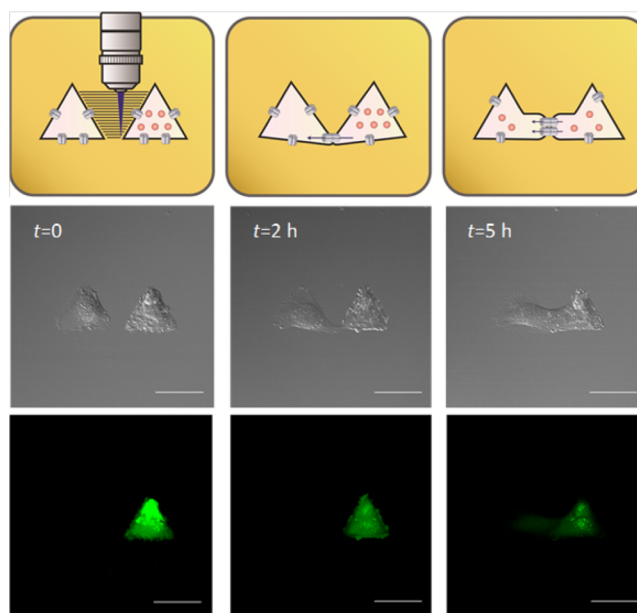


**Figure 8.** Monolayer presenting maltoheptaose-protected RGD ligands was photopatterned to give an array of  $1000 \mu\text{m}^2$  triangular features. After allowing HUVECs to attach and spread for several hours, patterned cells were located via imaging. A second triangular feature was illuminated at a set distance (center-to-center  $\sim 75 \mu\text{m}$ ) offset from existing cells. After culturing of a second population of HUVECs preloaded with calcein-AM dye, patterned cell pairs were located (left panel). The region in between cells was then irradiated to allow the cells to contact one another, and time-lapse imaging was used to observe the dynamics for cell–cell contact and diffusion of the dye through gap junctions. Bright-field and fluorescent images reveal the formation of cell–cell contact (middle panel) and subsequent calcein-AM dye transfer (right panel). Scale bar— $50 \mu\text{m}$ .

bridging gap junction channels; cells that were cultured without activation of the middle region showed no transfer. The ability to observe, in real time, the dynamics of cell–cell contact, gap junction formation, and transfer of molecules in individual cells offers a new opportunity for mechanistic studies of this important activity. More broadly, this experiment demonstrates the value of an intrinsically inert photoprotected RGD surface that can support repeated activation of ECM across multiple spatial and temporal scales.

## CONCLUSIONS

Dynamic surfaces having properties that can be modulated in real time offer a significant opportunity for understanding how cells respond to spatio-temporal changes in their micro-environments. We present here a dynamic SAM for repeated activation of RGD ligands that mediate cell adhesion. The use of light to activate the surface offers the greatest flexibility in spatio-temporal control over adhesion and allows repeated cycles of activation and cell attachment, which will be important for more complex experiments. The enablement of this strategy required that the monolayers are highly effective at preventing nonspecific adsorption of protein, and we found that the previous “gold standard” surfaces based on oligo(ethylene glycol) groups were insufficient. By using SPR to measure protein adsorption and cell culture experiments with patterned monolayers, we demonstrated that a revised protecting group that was modified with a maltoheptaose group met this requirement. The need for seven sugar units

(maltoheptaose) is likely due to the linear helical nature of the oligosaccharide, maximizing extension into the bulk phase but restricting the two-dimensional hydrophilic footprint, though further work will be required to determine the relevant mechanistic factors for this group. Nevertheless, we expect that the ability to laser-activate the RGD ligands on demand and sequentially will enable studies of cell behavior in response to multiple ECM cues (i.e., initiation of cell migration at diametrically opposing points) and cell–cell cues (i.e., hub cells induced to contact with two different receiver cells).

## ■ ASSOCIATED CONTENT

### 📄 Supporting Information

The Supporting Information is available free of charge on the ACS Publications website at DOI: [10.1021/acs.langmuir.8b04203](https://doi.org/10.1021/acs.langmuir.8b04203).

Experimental procedures, characterization data, and supplemental figures (PDF)

Time-lapse fluorescent microscopy of gap junction-mediated dye transfer after photoactivation (AVI)

## ■ AUTHOR INFORMATION

### Corresponding Author

\*E-mail: [milan.mrksich@northwestern.edu](mailto:milan.mrksich@northwestern.edu).

### ORCID

Milan Mrksich: [0000-0002-4964-796X](https://orcid.org/0000-0002-4964-796X)

### Notes

The authors declare no competing financial interest.

## ■ ACKNOWLEDGMENTS

The authors are grateful to Christopher Mauer (Nikon) for assistance with microscopy and Jennifer Grant for help with fabrication of the live-cell imaging chamber. Research reported in this publication was supported by the National Cancer Institute of the National Institutes of Health under award number U54CA199091. This work also made use of the IMSERC at Northwestern University, which has received support from the NIH (1S10OD012016-01/1S10RR019071-01A1), Soft and Hybrid Nanotechnology Experimental (SHyNE) Resource (NSF ECCS-1542205), and the State of Illinois and International Institute for Nanotechnology (IIN).

## ■ REFERENCES

- (1) Mrksich, M.; Whitesides, G. M. Using Self-Assembled Monolayers to Understand the Interactions of Man-made Surfaces with Proteins and Cells. *Annu. Rev. Biophys. Biomol. Struct.* **1996**, *25*, 55–78.
- (2) Roberts, C.; Chen, C. S.; Mrksich, M.; Martichonok, V.; Ingber, D. E.; Whitesides, G. M. Using Mixed Self-Assembled Monolayers Presenting RGD and (EG)3OH Groups To Characterize Long-Term Attachment of Bovine Capillary Endothelial Cells to Surfaces. *J. Am. Chem. Soc.* **1998**, *120*, 6548–6555.
- (3) Raynor, J. E.; Capadona, J. R.; Collard, D. M.; Petrie, T. A.; García, A. J. Polymer brushes and self-assembled monolayers: Versatile platforms to control cell adhesion to biomaterials (Review). *Biointerphases* **2009**, *4*, FA3–FA16.
- (4) Mrksich, M. Using self-assembled monolayers to model the extracellular matrix. *Acta Biomater.* **2009**, *5*, 832–841.
- (5) Gooding, J. J.; Parker, S. G.; Lu, Y.; Gaus, K. Molecularly Engineered Surfaces for Cell Biology: From Static to Dynamic Surfaces. *Langmuir* **2014**, *30*, 3290–3302.
- (6) Rosales, A. M.; Anseth, K. S. The design of reversible hydrogels to capture extracellular matrix dynamics. *Nat. Rev. Mater.* **2016**, *1*, 15012.
- (7) Robertus, J.; Browne, W. R.; Feringa, B. L. Dynamic control over cell adhesive properties using molecular-based surface engineering strategies. *Chem. Soc. Rev.* **2010**, *39*, 354–378.
- (8) Nakanishi, J. Switchable Substrates for Analyzing and Engineering Cellular Functions. *Chem.—Asian J.* **2013**, *9*, 406–417.
- (9) Koçer, G.; Jonkheijm, P. About Chemical Strategies to Fabricate Cell-Instructive Biointerfaces with Static and Dynamic Complexity. *Adv. Healthcare Mater.* **2018**, *7*, 1701192.
- (10) Yeo, W.-S.; Yousaf, M. N.; Mrksich, M. Dynamic Interfaces between Cells and Surfaces: Electroactive Substrates that Sequentially Release and Attach Cells. *J. Am. Chem. Soc.* **2003**, *125*, 14994–14995.
- (11) Chan, E. W. L.; Yousaf, M. N. Immobilization of Ligands with Precise Control of Density to Electroactive Surfaces. *J. Am. Chem. Soc.* **2006**, *128*, 15542–15546.
- (12) Yang, J.; Yamato, M.; Okano, T. Cell-Sheet Engineering Using Intelligent Surfaces. *MRS Bull.* **2005**, *30*, 189–193.
- (13) Wong, D. S. H.; Li, J.; Yan, X.; Wang, B.; Li, R.; Zhang, L.; Bian, L. Magnetically Tuning Tether Mobility of Integrin Ligand Regulates Adhesion, Spreading, and Differentiation of Stem Cells. *Nano Lett.* **2017**, *17*, 1685–1695.
- (14) Mendes, P. M. Stimuli-responsive surfaces for bio-applications. *Chem. Soc. Rev.* **2008**, *37*, 2512–2529.
- (15) Pulsipher, A.; Yousaf, M. N. Surface Chemistry and Cell Biological Tools for the Analysis of Cell Adhesion and Migration. *ChemBioChem* **2010**, *11*, 745–753.
- (16) Prime, K. L.; Whitesides, G. M. Adsorption of proteins onto surfaces containing end-attached oligo(ethylene oxide): a model system using self-assembled monolayers. *J. Am. Chem. Soc.* **1993**, *115*, 10714–10721.
- (17) Nakanishi, J.; Kikuchi, Y.; Takarada, T.; Nakayama, H.; Yamaguchi, K.; Maeda, M. Spatiotemporal control of cell adhesion on a self-assembled monolayer having a photocleavable protecting group. *Anal. Chim. Acta* **2006**, *578*, 100–104.
- (18) Shimizu, Y.; Kamimura, M.; Yamamoto, S.; Abdellatif, S. A.; Yamaguchi, K.; Nakanishi, J. Facile Preparation of Photoactivatable Surfaces with Tuned Substrate Adhesiveness. *Anal. Sci.* **2016**, *32*, 1183–1188.
- (19) Park, S.; Yousaf, M. N. An Interfacial Oxime Reaction To Immobilize Ligands and Cells in Patterns and Gradients to Photoactive Surfaces. *Langmuir* **2008**, *24*, 6201–6207.
- (20) Wirkner, M.; Weis, S.; San Miguel, V.; Álvarez, M.; Gropeanu, R. A.; Salierno, M.; Sartoris, A.; Unger, R. E.; Kirkpatrick, C. J.; del Campo, A. Photoactivatable Caged Cyclic RGD Peptide for Triggering Integrin Binding and Cell Adhesion to Surfaces. *ChemBioChem* **2011**, *12*, 2623–2629.
- (21) Houseman, B. T.; Gawalt, E. S.; Mrksich, M. Maleimide-Functionalized Self-Assembled Monolayers for the Preparation of Peptide and Carbohydrate Biochips. *Langmuir* **2003**, *19*, 1522–1531.
- (22) Sobers, C. J.; Wood, S. E.; Mrksich, M. A gene expression-based comparison of cell adhesion to extracellular matrix and RGD-terminated monolayers. *Biomaterials* **2015**, *52*, 385–394.
- (23) Hersel, U.; Dahmen, C.; Kessler, H. RGD modified polymers: biomaterials for stimulated cell adhesion and beyond. *Biomaterials* **2003**, *24*, 4385–4415.
- (24) Su, J.; Mrksich, M. Using Mass Spectrometry to Characterize Self-Assembled Monolayers Presenting Peptides, Proteins, and Carbohydrates. *Angew. Chem., Int. Ed.* **2002**, *41*, 4715–4718.
- (25) Mrksich, M.; Sigal, G. B.; Whitesides, G. M. Surface Plasmon Resonance Permits In Situ Measurement of Protein Adsorption on Self-Assembled Monolayers of Alkanethiolates on Gold. *Langmuir* **1995**, *11*, 4383–4385.
- (26) Sigal, G. B.; Mrksich, M.; Whitesides, G. M. Effect of Surface Wettability on the Adsorption of Proteins and Detergents. *J. Am. Chem. Soc.* **1998**, *120*, 3464–3473.
- (27) Ostuni, E.; Chapman, R. G.; Holmlin, R. E.; Takayama, S.; Whitesides, G. M. A Survey of Structure–Property Relationships of

Surfaces that Resist the Adsorption of Protein. *Langmuir* **2001**, *17*, 5605–5620.

(28) Luk, Y.-Y.; Kato, M.; Mrksich, M. Self-Assembled Monolayers of Alkanethiolates Presenting Mannitol Groups Are Inert to Protein Adsorption and Cell Attachment. *Langmuir* **2000**, *16*, 9604–9608.

(29) Alang Ahmad, S. A.; Wong, L. S.; ul-Haq, E.; Hobbs, J. K.; Leggett, G. J.; Micklefield, J. Protein Micro- and Nanopatterning Using Aminosilanes with Protein-Resistant Photolabile Protecting Groups. *J. Am. Chem. Soc.* **2011**, *133*, 2749–2759.

(30) Tanaka, T.; Nagai, H.; Noguchi, M.; Kobayashi, A.; Shoda, S.-i. One-step conversion of unprotected sugars to  $\beta$ -glycosyl azides using 2-chloroimidazolinium salt in aqueous solution. *Chem. Commun.* **2009**, 3378–3379.